Theory of Spin-Conserving Excitation of the N – V – Center in Diamond

Theory of spin-conserving excitation of the $N - V^-$ center in diamond

Adam Gali,[1,2] Erik Janzén,[3] Péter Deák,[4] Georg Kresse,[5] and Efthimios Kaxiras[2]

[1]*Department of Atomic Physics, Budapest University of Technology and Economics, Budafoki út 8., H-1111, Budapest, Hungary*
[2]*Department of Physics and School of Engineering and Applied Sciences, Harvard University, Cambridge, MA 02138, USA*
[3]*Department of Physics, Chemistry and Biology, Linköping University, S-581 83 Linköping, Sweden*
[4]*Bremen Center for Computational Materials Science, Universität Bremen, Am Fallturm 1, 28359 Bremen, German*
[5]*Institut für Materialphysik, Universität Wien, Sensengasse 8/12, 1090 Wien, Austria*

The negatively charged nitrogen-vacancy defect ($N - V^-$ center) in diamond is an important atomic-scale structure that can be used as a qubit in quantum computing and as a marker in biomedical applications. Its usefulness relies on the ability to optically excite electrons between well-defined gap states, which requires clear and detailed understanding of the relevant states and excitation processes. Here we show that by using hybrid density-functional-theory calculations in a large supercell we can reproduce the zero-phonon line and the Stokes and anti-Stokes shifts, yielding a complete picture of the spin-conserving excitation of this defect.

Quantum computing and its many exciting applications relies on the successful realization of quantum logic bits (qubits) that can operate under practically feasible conditions. Few physical systems can meet the requirements of controlled quantum coherence and robust operational conditions. One of the most promising candidates is the negatively charged nitrogen-vacancy defect ($N - V^-$ center) in bulk diamond [1, 2]: the spin state of this defect can be manipulated using excitation from the $^3A_2$ ground state to the ^3E excited state by optical absorption (Fig. 1). The main advantage of the $N - V^-$ center is that it can operate at *room temperature* as a solid state qubit [3, 4, 5, 6, 7, 8, 9]. Detailed understanding of this excitation process is crucial in the realization of qubits based on diamond. However, achieving this level of understanding stretches the capabilities of theoretical methods that are usually applied to the study of defects in solids because of the special nature of the $N - V^-$ defect. Specifically, this defect combines strong coupling of ionic and electronic degrees of freedom with a many-body character of the electronic states, and its interpretation is further complicated by contradictory experimental measurements of the emission spectrum at different temperatures [2, 10].

In this Letter, we report a theoretical investigation of the radiative transitions of the $N - V^-$ center using electronic structure calculations, which give a consistent and accurate account of the excitations observed and provide a plausible resolution of the experimental situation. We utilized the HSE06 screened Hartree–Fock hybrid exchange-correlation density functional [11, 12] to determine the geometry and excitation energies of the $N - V^-$ center, and we compare the results to the traditional PBE [13] exchange-correlation density functional and the experimental data. We find that – in contrast to PBE – the HSE06 functional (which reproduces the band gap of diamond within 0.5%), can also reproduce both the zero-phonon line and the Stokes-shift quantitatively (within 1.5% in this case). This result demonstrates that hybrid functionals improve not only the excitation of the extended system (gap) but also localized ones. This promises a very significant advantage in defect calculations. Motivated by the success of the hybrid functional to reproduce key experimental measurements of the excitation process, we calculate an anti-Stokes shift of 0.217 eV, measured to be 0.185 eV at usual experimental conditions at low temperature [2]. From this result, we argue that the anti-Stokes shift of 0.065 eV measured at low temperature under high-energy-density laser illumination [10], is most likely due to the local heating of the sample caused by the focused laser beam.

Previous density functional theory (DFT) calculations have shown [14, 15, 16, 17] that well defined defect levels appear in the band gap due to this defect: a fully occupied a_1 level and a doubly occupied two-fold degenerate e-level at a higher energy. The electrons have parallel spins on the e-level preserving the C_{3v} symmetry of the defect; a many-body wavefunction built from single-particle states in the gap represents the $^3A_2$ ground state. The excitation can be understood as promoting one electron from the a_1 level to the e level resulting in a new many-body excited state, ^3E, as shown schematically in Fig. 1.

Excitation changes not only the electron wavefunction but the atomic structure of the defect as well. Hence, the ground state and the excited state will possess different potential energy surfaces (PES) and different vibrational states, as shown schematically in Fig. 2. The transition between the lowest PES will result in the zero-phonon line (ZPL) both in absorption and emission, a process in which no real phonons are involved in the excitation or de-excitation process. The ZPL was measured at 1.945 eV (yellow light) both in low temperature absorption and emission [2]. At liquid-nitrogen tempera-

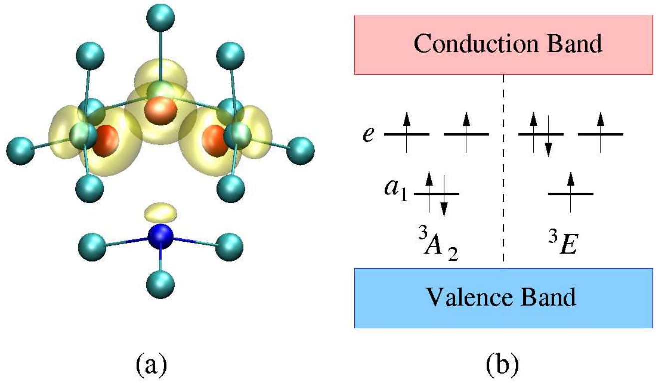

FIG. 1: (Color online) (a) The structure of $N - V^{-}$ center in diamond; only first- and second-neighbor C (cyan spheres) and N (blue sphere) atoms to the vacant site are shown. The yellow and red lobes are contours of the calculated difference in spin density for the ^3E state as obtained by the HSE06 and PBE functionals. (b) Schematic diagram of the defect states in the gap and their occupation in the $^3A_2$ (ground) and ^3E (excited) states.

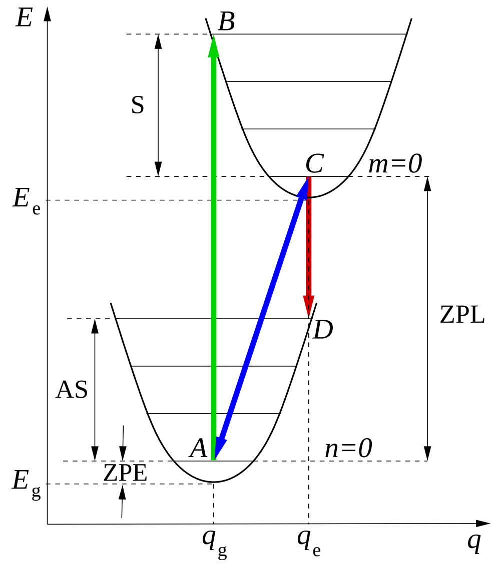

FIG. 2: (Color online) The energy (E) vs. configuration coordinate (q) diagram for the excitation process of a defect in the Franck-Condon approximation: $E_{\rm g}$, $E_{\rm e}$ are the minima in the quasi-parabolic potential energy surfaces of the defect in the ground and excited states, respectively and $q_{\rm g}$, $q_{\rm e}$ the corresponding coordinates. ZPE is the zero point energy (indicated only for the ground state). The energy ladders show the phonon energies with the phonon ground states at $n = 0$ (ground state of the defect) and $m = 0$ (excited state). At elevated temperatures the high-energy phonon states can be occupied by inducing transition $A \to B$ (vertical absorption, green arrow), and $C \to D$ (vertical emission, red arrow). Transition $A \leftrightarrow C$ corresponds to the zero-phonon line (ZPL, blue double arrow) both in absorption and emission. The energy of the Stokes shift (S) and anti-Stokes shift (AS) are also shown.

ture a broad phonon side band was measured in absorption with phonon-related peaks at approximately 2.020, 2.110, 2.180 and 2.250 eV, with the highest intensity at 2.180 eV (green light), while in the emission band the first phonon sidebands, better resolved than in absorption, are found at 1.880, 1.820, and 1.760 eV, with the 1.760 eV peak (red light) having the highest intensity [2].

The Franck–Condon approximation is commonly used to interpret the excitation spectrum, that is, assuming that the electronic transition is very fast compared with the motion of nuclei in the lattice. In addition to the Franck–Condon assumption, three other approximations are commonly assumed (see Fig. 2). The first is that each lattice vibrational mode is well described by a quantum harmonic oscillator, as implied by the quasi-parabolic shape of the potential wells, and almost constant energy spacing between phonon energy levels. The second, called the low-temperature approximation, is that only the lowest (zero-point) lattice vibration is excited, implying that electronic transitions do not originate from any of the higher phonon levels. The third, called the linear-coupling approximation, is that the interaction between the defect and the lattice is the same in both the ground and the excited states; this implies two equally shaped parabolic potentials and equally spaced phonon energy levels in both the ground and excited states. The detected phonon peaks in the spectrum may be associated with the $m = 1, 2, \ldots$ and $n = 1, 2, \ldots$ quanta of a characteristic phonon mode in absorption and emission.

The highest intensity in the phonon side band at low temperatures corresponds to the excitations where the geometry does not change, that is, the vertical absorption and emission [18]. This way the Stokes and anti-Stokes shifts are determined, which reveal the relaxation energy of the atoms due to the electronic excitation (see Fig. 2). In the linear coupling approximation the Stokes and anti-Stokes shifts would have the same value but experimental measurements indicate a difference of about 0.05 eV (see Table I and related discussion).

Another complication in understanding the excitation and de-excitation processes arises from a recent measurement [10] of the highest emission intensity in the phonon sideband at ≈1.880 eV. In this measurement, the second peak at 1.820 eV is clearly visible but the third at 1.760 eV is almost missing [10]. This measurement was carried out at 10 K. This is puzzling since at higher temperature (for instance, at liquid nitrogen temperature, 77 K, where earlier experiments were conducted [2]), higher-energy phonon states can be occupied resulting in larger vertical emission energy, the opposite of what was found in the recent measurements [10]. We note that in the latter, low-temperature (10 K) experiment, a laser beam was focused with a 10 cm lens, increasing the energy density by a factor of 10^4. In fact, this experiment measured the ionization of $N - V^-$ defects from the ^3E excited state during the high intense excitation [10]. Assuming that all the usual approximations hold for this process, an anti-Stokes shift of 0.065 eV can be deduced [10] which clearly contradicts the results of earlier experiments [2]. This issue must be addressed and resolved in a full explanation of the process.

State-of-the-art methods to investigate defect properties in solids employ DFT in a supercell geometry. While the calculation of the ground state charge and spin density can be obtained accurately using the local density approximation (LDA) for the exchange-correlation functional or by other functionals that include density-gradient corrections (for example, the PBE functional [13]), the accurate calculation of the excitation energies presents a challenging problem due to the well-known self-interaction error of these methods. For example, the LDA value for the zero-phonon line (ZPL) of the $N - V^-$ center is 1.71 eV [15] compared to the experimental data, 1.945 eV [2]. The Bethe-Salpeter equation followed by the parameter-free GW-method for the quasi-particle correction of the Kohn-Sham levels [19] is the best tool to calculate the excitation energies, but it is computationally prohibitive for large supercells. Recently, it was shown that both the band gap [20] and the excitation energies [21] are vastly improved by applying a screened Hartree–Fock hybrid density functional [11, 12], referred to as the HSE06 hybrid functional.

We employed two methods to calculate the excitation properties of the $N - V^-$ center in diamond: the traditional PBE functional and the HSE06 hybrid functional. First, the diamond primitive lattice was optimized, then a simple cubic 512-atom supercell was constructed. Finally, we placed the negatively charged nitrogen-vacancy defect in the supercell, and optimized the structure for each given electronic configuration. We employed the VASP5.1 code [22] to carry out these calculations with a plane-wave basis set (using an energy cut-off of 420 eV) and PAW-type potentials to model the atomic cores [23, 24]. For the optimization of the lattice constant we used a plane-wave cut-off energy of 840 eV and a $12 \times 12 \times 12$ Monkhorst–Pack k-point set [25] for the primitive diamond lattice. For the 512-atom supercell we used the Γ-point that provides a well-converged charge density. We note here that all these calculations use the Born–Oppenheimer approximation, so the electron states are calculated as a function of the coordinates of the nuclei treated as classical particles. This approximation is valid at low temperatures.

The calculated lattice constant of diamond is slightly different in the PBE (3.567 Å) and the HSE06 (3.545 Å) approximations. The calculated band gap is very different in the two approaches: the PBE functional yields 4.16 eV, while the HSE06 functional gives 5.43 eV, very close to the experimental value of 5.48 eV. The PBE-functional error is large both in absolute value (1.32 eV) and relative value (24.1%); these values are reduced by the HSE06 functional to 0.05 eV and 1.0%, respectively. We expect that the calculated excitation energies of the defect excited states will be also improved by using hybrid functionals [26, 27, 28].

TABLE I: The calculated vertical absorption ($A \to B$) and vertical emission energies ($C \to D$), and the zero-phonon line (ZPL) obtained with the PBE and HSE06 functionals, compared to measured values from Ref. [2]. The Stokes-shift (S) between the vertical absorption and the ZPL, and the anti-Stokes-shift (AS) between the ZPL and the vertical emission are also given (all values in eV).

	ZPL	$A \to B$	S	$C \to D$	AS
PBE	1.706	1.910	0.204	1.534	0.172
HSE06	1.955	2.213	0.258	1.738	0.217
Exp. [2]	1.945	2.180	0.235	1.760	0.185

The $^3A_2$ ground state of the $N - V^-$ center is obtained by spin polarized calculations both with the PBE and HSE06 functionals. The ^3E excited state is simply obtained by promoting one electron from the a_1 defect level to the e defect level in the band gap [14, 15]. In the VASP code it is possible to set the occupation numbers of the single particle levels, thus the ^3E excited state can be calculated in a self-consistent manner through such constrained occupation. The total energy was minimized for both electronic configurations as a function of the coordinates of the nuclei, which allows us to determine the configuration coordinates of the ground state (q_g) and the excited state (q_e) of the defect. The corresponding energy minima in the calculations are shown as E_g and E_e in Fig. 2. The zero-point vibration states ($n = 0$ and $m = 0$) will raise these energies by a value of order a few tens meV, called zero-point energy (ZPE, shown in Fig. 2); for example, Davies and Hamer [2] deduced a ZPE value of ≈35 meV. We note that the difference between the ZPE values of E_g and E_e is expected to be even smaller, of order a few meV. The energy difference between the energy minima of E_g and E_e therefore gives a very good estimate of the ZPL ($A \to C$ transition, see Fig. 2). The transitions $A \to B$ and $C \to D$ are readily calculated by fixing the geometry at q_g and q_e, respectively, while varying the electronic configurations as explained above. We note that the error associated with the ZPE cannot be avoided in the calculated $A \to B$ and $C \to D$ transitions, which means that the values for these transitions are less accurate than for the ZPL. The calculated excitation energies using the PBE and HSE06 functionals are given in Table I.

The PBE functional gives too low value for the ZPL (≈1.71 eV), so this gradient corrected functional does not improve the LDA value (1.71 eV [15]) at all. This is not surprising since both the LDA and the PBE functionals suffer from the self-interaction error. However, the HSE06 functional gives an almost perfect value, the difference from experiment being smaller than 0.5%. Apparently, the HSE06 functional improves not just the band gap of the perfect semiconductor but the defect internal transition energy as well. The PBE functional does not improve the LDA values for the vertical absorption energy either, which is again too low by ≈0.3 eV. The HSE06 functional yields an almost perfect value for the energy of the vertical absorption compared to the experimental result (within 1.4%). The larger discrepancy for the $A \rightarrow B$ transition than for the ZPL may be attributed to the intrinsic ZPE error as explained above. We note that the calculated Stokes shift (the relaxation energy), is close to the experimental result from both the PBE and the HSE06 functionals. The reason is that the self-interaction error inherent in the PBE functional is almost fully canceled, as the relaxation energy corresponds to the energy difference between two different atomic configurations with the same electronic configuration. The wavefunctions and the spin density obtained with the HSE06 functional are somewhat more localized than those obtained with the PBE functional. For example, the integrated spin density of the ^3E state in a 5^3 Å^3 cube centered at the vacant site containing the three carbon atoms and the nitrogen atom is 1.61 and 1.64 obtained in PBE and HSE06 calculations, respectively (see Fig. 1). This is expected of the HSE06 functional which contains the Hartree–Fock exchange, giving more localized wave functions than the pure DFT-PBE.

Having established the high level of accuracy of the HSE06 functional, we can address the issue of the vertical emission energy and the anti-Stokes shift. The value calculated with the PBE functional is again very low and not comparable to any experimental data. However, the HSE06 value (1.738 eV) is very close to the measurement of Davies and Hamer (1.760 eV) [2]. Since our calculations are valid at low temperature we assume that the low temperature approximation beyond the Franck–Condon assumption holds for this transition. We conclude that the anti-Stokes shift is 0.185 eV at usual experimental conditions at low temperatures for the $N-V^-$ defect in diamond. For this defect the linear-coupling approximation does not hold. The difference between the Stokes and anti-Stoke shifts is ≈(0.235-0.185) eV=0.050 eV in experiment, which compares favorably to the HSE06 value (0.258-0.217) eV=0.041 eV. This indicates somewhat different shape of the PES for the ground state and the excited state, thus different vibration modes.

The only remaining unresolved issue is the recent experiment suggesting a much lower anti-Stokes value of 0.065 eV [10]. We suggest that the high energy density excitation in this experiment resulted in local heating of the sample in the area where the laser beam was focused. The local heating of the sample will break the low temperature approximation and will cause a shift in the occupation of the phonon states from $m = 0$ to $m = 2$. That may explain why the detected vertical emission energy is larger at 10 K (at high energy density) than at 77 K (at low energy density) excitation. Our results indicate that detailed analysis of the vibration modes of the ^3E excited state is important for a complete understanding of the radiative emission of the $N-V^-$ center; further experimental and theoretical efforts are needed in this direction.

AG acknowledges support from Hungarian OTKA No. K-67886 and the grant of SNIC001-08-175 from the Swedish National Supercomputer Center; we thank Jeronimo Maze for fruitful discussions.

[1] L. du Preez, PhD. dissertation, University of Witwatersrand, 1965.
[2] G. Davies and M. F. Hamer, Proc. R. Soc. London Ser. A **348**, 285 (1976).
[3] J. Wrachtrup, S. Y. Kilin, and A. P. Nizotsev, Opt. Sepctrosc. **91**, 429 (2001).
[4] F. Jelezko *et al.*, Phys. Rev. Lett. **93**, 130501 (2004).
[5] R. J. Epstein, F. Mendoza, Y. K. Kato, and D. D. Awschalom, Nat. Phys. **1**, 94 (2005).
[6] R. Hanson, F. M. Mendoza, R. J. Epstein, and D. D. Awschalom, Phys. Rev. Lett. **97**, 087601 (2006).
[7] L. Childress *et al.*, Science **314**, 281 (2006).
[8] M. V. Gurudev Dutt *et al.*, Science **316**, 312 (2007).
[9] R. Hanson *et al.*, Science **320**, 352 (2008).
[10] N. B. Manson and J. P. Harrison, Diam. and Rel. Mater. **14**, 1705 (2005).
[11] J. Heyd, G. E. Scuseria, and M. Ernzerhof, The Journal of Chemical Physics **118**, 8207 (2003).
[12] A. V. Krukau, O. A. Vydrov, A. F. Izmaylov, and G. E. Scuseria, The Journal of Chemical Physics **125**, 224106 (2006).
[13] J. P. Perdew, K. Burke, and M. Ernzerhof, Phys. Rev. Lett. **77**, 3865 (1996).
[14] J. P. Goss *et al.*, Phys. Rev. Lett. **77**, 3041 (1996).
[15] A. Gali, M. Fyta, and E. Kaxiras, Phys. Rev. B **77**, 155206 (2008).
[16] J. A. Larsson and P. Delaney, Phys. Rev. B **77**, 165201 (2008).
[17] F. M. Hossain, M. W. Doherty, H. F. Wilson, and L. C. L. Hollenberg, Phys. Rev. Lett. **101**, 226403 (2008).
[18] K. Huang and A. Rhys, Proc. Roy. Soc. A **204**, 406 (1950).
[19] L. Hedin and S. Lundqvist, in *Solid State Physics*, edited by H. Ehrenreich, F. Seitz, and D. Turnbull (Academic, New York, 1969), Vol. 23.
[20] M. Marsman, J. Paier, A. Stroppa, and G. Kresse, Journal of Physics: Condensed Matter **20**, 064201 (9pp) (2008).
[21] J. Paier, M. Marsman, and G. Kresse, Physical Review B **78**, 121201 (2008).
[22] G. Kresse and J. Furthmüller, Phys. Rev. B **54**, 11169 (1996).
[23] P. E. Blöchl, Phys. Rev. B **50**, 17953 (1994).
[24] G. Kresse and D. Joubert, Phys. Rev. B **59**, 1758 (1999).
[25] H. J. Monkhorst and J. K. Pack, Phys. Rev. B **13**, 5188 (1976).
[26] P. Deák *et al.*, Journal of Physics: Condensed Matter **17**,

S2141 (2005).
[27] A. Alkauskas, P. Broqvist, and A. Pasquarello, Phys. Rev. Lett. **101**, 046405 (2008).
[28] P. Deák, B. Aradi, T. Frauenheim, and A. Gali, Materials Science and Engineering B **154-155**, 187 (2008).